

Phenylpropanoid glycosides from the fruit of *Lycium barbarum* L. and their bioactivity

Qing-Wen Li^{a,1}, Rui Zhang^{b,1}, Zheng-Qun Zhou^{a,c,**}, Wan-Yang Sun^a, Hong-Xia Fan^{a,c}, Ying Wang^d, Jia Xiao^b, Kwok-Fai So^e, Xin-Sheng Yao^a, Hao Gao^{a,*}

^a Institute of Traditional Chinese Medicine and Natural Products, College of Pharmacy / Guangdong Province Key Laboratory of Pharmacodynamic Constituents of TCM and New Drugs Research, Jinan University, Guangzhou 510632, People's Republic of China

^b Clinical Medicine Research Institute, The First Affiliated Hospital of Jinan University, Guangzhou 510632, People's Republic of China

^c Integrated Chinese and Western Medicine Postdoctoral Research Station, Jinan University, Guangzhou 510632, People's Republic of China

^d Guangdong Provincial Key Laboratory of Applied Botany, South China Botanical Garden, Chinese Academy of Sciences, Guangzhou 510650, People's Republic of China

^e Guangdong Medical Key Laboratory of Brain Function and Diseases, GMH Institute of Central Nervous System Regeneration, Jinan University, Guangzhou, 510632, People's Republic of China

ARTICLE INFO

Keywords:

Lycium barbarum L. (Solanaceae)

Goji

Wolfberry

Phenylpropanoid glycosides

Antioxidant activity

Hypoglycemic activity

ABSTRACT

Fifteen phenylpropanoid glycosides, including six undescribed compounds were isolated from the fruit of *Lycium barbarum* L. (Solanaceae) (goji or wolfberry). Their structures were identified by detailed spectroscopic analyses. Seven known compounds were firstly isolated from the genus *Lycium*, in which the 1D and 2D NMR data of one compound were reported for the first time. Notably, two undescribed compounds were a pair of rare tautomeric glycoside anomers characterized by the presence of free anomeric hydroxy. Antioxidant and hypoglycemic activities of all these compounds were assessed using DPPH radical scavenging, oxygen radical absorbance capacity (ORAC), and α -glucosidase inhibitory assays, respectively. These compounds showed different levels of oxygen radical absorbance capacity, and some isolates exhibited potent antioxidant activity with greater ORAC values than the positive control (EGCG).

1. Introduction

Lycium barbarum L. (Solanaceae) is a deciduous woody perennial plant that grows in northwestern China and other parts of Asia, and its ripe fruits (which are named goji or wolfberry) are 1–2 cm-long bright red ellipsoid berries (Amagase and Farnsworth, 2011). Goji has been used widely as a functional food and traditional Chinese medicine (TCM) for replenishing vital essence to improve eyesight and nourish the liver and kidneys (Qian et al., 2017). Modern pharmacological studies suggested that goji exhibited various activities, such as antioxidant, antitumor, hypoglycemic, and anti-Alzheimer's disease properties (Wojdyło et al., 2018; Zhou et al., 2016b). Glycosides are the most abundant natural products in goji, including phenylpropanoid, coumarin, lignan, flavonoid, and dicaffeoylspermidine glycosides (Zhou et al., 2016a,b; Zhou et al., 2017; Gao and Yao, 2019). Glycosides occur widely in plants, microorganisms, and animals. Usually, the sugar

moieties are added onto the aglycones at the post-modification stage via stepwise glycosylation with various glycosyltransferases, which catalyze glycosidic bond formation between a sugar and acceptor (Yang et al., 2015; Kulkarni et al., 2018).

In our previous chemical study on goji, some phenylpropanoid glycosides were isolated (Zhou et al., 2017). This present phytochemical study with a larger scale led to the discovery of fifteen phenylpropanoid glycosides (1–15) (Fig. 1), including six undescribed compounds (1–6) and seven known compounds firstly reported from the genus *Lycium*. Compounds 1 and 2 were obtained as a pair of inseparable anomers due to the tautomerism of the hemiacetal at C-1' in solution. Considering the biological activities of goji and the relationship between hyperglycemia and oxidative tissue damage, antioxidant and α -glucosidase inhibitory activities of compounds 1–15 were evaluated (Amagase and Farnsworth, 2011; Zhou et al., 2016b, 2017; Cardullo et al., 2019). Details of isolation, structural identification, and

* Corresponding author.

** Corresponding author. Institute of Traditional Chinese Medicine and Natural Products, College of Pharmacy / Guangdong Province Key Laboratory of Pharmacodynamic Constituents of TCM and New Drugs Research, Jinan University, Guangzhou, 510632, People's Republic of China.

E-mail addresses: tzhouzq@jnu.edu.cn (Z.-Q. Zhou), tghao@jnu.edu.cn (H. Gao).

¹ These authors contributed equally to this work.

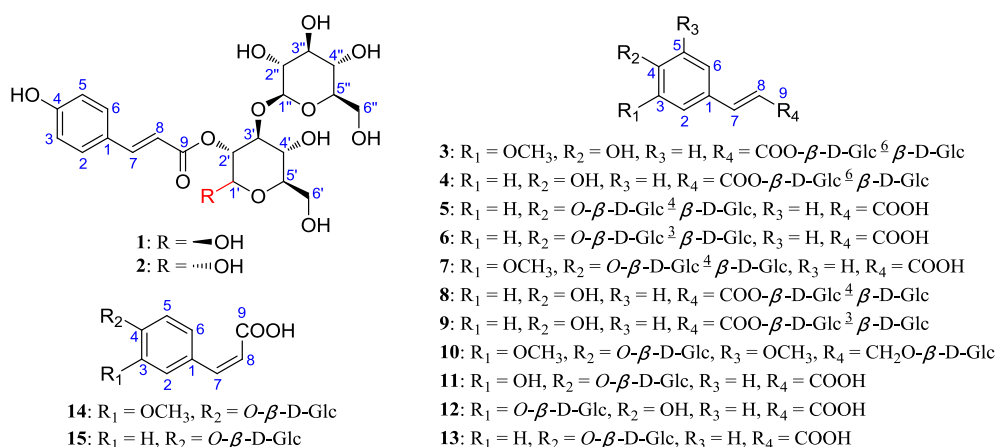


Fig. 1. Chemical structures of compounds 1–15.

biological effects of 1–15 are reported in this paper.

2. Results and discussion

Compounds 1 and 2 were obtained as yellowish amorphous powders and are tautomeric and coexist in solution. The quasi-molecular ion at m/z 511.1426 $[M + Na]^+$ by HR-ESI-MS showed that the molecular formulas of 1 and 2 were C₂₁H₂₈O₁₃ (eight indices of hydrogen deficiency). The NMR spectra of the mixture of 1 and 2 showed two sets of signals, and the corresponding integral area ratios of ¹H NMR signals of 1 and 2 were approximately 1:3 (Figure S1, Supporting Information). The ¹³C NMR spectrum of 1/2 displayed 21 carbons. Based on the DEPT-135 data, these carbons could be categorized as one carbonyl, eight aromatic or olefinic carbons (including six sp² methine carbons), 10 oxygenated sp³ methine carbons, and two oxygenated sp³ methylene carbons. The ¹H NMR spectrum of 1/2 exhibited six aromatic or olefinic protons and a set of glycosyl protons. The proton signals were associated with the directly attached carbon atoms in the HSQC experiment. The analysis of the ¹H–¹H COSY experiment and the coupling values of the protons exhibited the presence of five subunits [C-2–C-3, C-5–C-6, C-7–C-8, C-1'–C-2'–C-3'–C-4'–C-5'–C-6', and C-1''–C-2''–C-3''–C-4''–C-5''–C-6'']. Based on these deduced subunits, molecular formulas, and degrees of unsaturation, the key HMBC correlations shown in Fig. 2 determined the planar structures of 1/2. The assignments of all proton and carbon resonances are provided in Table 1.

The planar structures of 1 and 2 exhibited two pyranohexose units. Based on the coupling values (1: $J_{1'-2'} = 8.0$ Hz, $J_{2'-3'} = 9.5$ Hz, $J_{3'-4'}/J_{4'-5'} = 9.6/8.8$ Hz; 2: $J_{1'-2'} = 3.6$ Hz, $J_{2'-3'}/J_{3'-4'}/J_{4'-5'} = 9.0/9.8$ Hz), the inside pyranohexose units of 1 and 2 were established as glucopyranosyls, and their relative configurations were identified as β (1) and α (2), respectively. A precise comparison of ¹³C NMR data of the sugar unit with those of glycosides recorded in the literature (Zhou et al., 2017; Bock and Pedersen, 1983) and the coupling values (1: $J_{1'-2'} = 8.0$ Hz; 2: $J_{1'-2'} = 8.0$ Hz) indicated that the outside pyranohexose units of 1 and 2 were also glucopyranosyls, and both the relative configurations of glucopyranosyls were β. The absolute configurations of

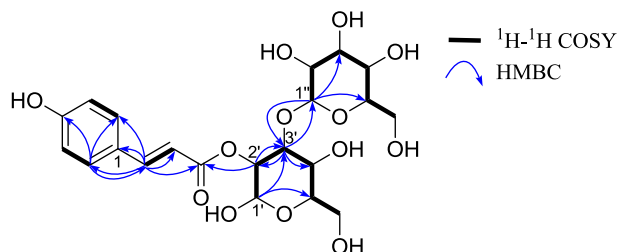


Fig. 2. Key 2D NMR correlations of compounds 1/2.

the glucopyranosyls were determined by HPLC analysis of products obtained from acid hydrolysis and derivatization reactions by L-cysteine methyl ester hydrochloride and *o*-tolyl isothiocyanate (Tanaka et al., 2007). Analytical HPLC was performed on the Phenomenex Gemini C₁₈ column with isocratic elution of CH₃CN–H₂O–HCOOH (25:75:0.1, v/v/v) for 40 min at a flow rate of 0.8 mL/min, and the peaks of the standard monosaccharide and sample derivatives were recorded at t_R 20.4 (D-Glc), 18.7 (L-Glc), and 20.4 (1/2) min, respectively. This evidence revealed that the two glucopyranosyls of 1/2 were D-Glc. Therefore, compounds 1 and 2 were established as 2-*O*-*trans*-p-coumaroyl-3-*O*-β-D-glucopyranosyl-β-D-glucopyranoside (named lycibarbarphenylpropanoid J) and 2-*O*-*trans*-p-coumaroyl-3-*O*-β-D-glucopyranosyl-α-D-glucopyranoside (named lycibarbarphenylpropanoid K), respectively.

Due to the tautomerism of the hemiacetal at C-1', compounds 1 and 2 coexisted as a pair of inseparable anomers in solution (Fig. 3) (Sun et al., 2016; Chen et al., 2013). As shown in Fig. 3, the peaks of 1 and 2 were observed at t_R 9.0 and 10.2 min (Phenomenex Gemini C₁₈ column, 4.6 × 250 mm², 5 μm; CH₃CN–H₂O–HCOOH 10:90:0.1, v/v/v, flow rate 1.0 mL/min; 280 nm), respectively, and their relative peak area ratio (27.6% for 1 and 72.4% for 2) in the HPLC chromatogram was approximately 1:3, which was corresponded to those of protons resonances of 1 and 2.

Compound 3 was obtained as a yellowish amorphous powder. The molecular formula of 3 was determined as C₂₂H₃₀O₁₄ by HR-ESI-MS (m/z 541.1533 $[M + Na]^+$; calcd. for C₂₂H₃₀O₁₄Na, 541.1533). The detailed analyses of 1D/2D NMR data of 3 (Table S3, Supporting Information) determined a planar structure consisting of *trans*-feruloyl and two pyranohexose units. A precise comparison of ¹³C NMR data of the sugar unit with those of glycosides recorded in the literature (Bock and Pedersen, 1983; Usui et al., 2017) and the coupling values ($J_{1'-2'} = 7.0$ Hz, $J_{1''-2''} = 7.8$ Hz) indicated that the sugar chain of 3 was glucopyranosyl-(1 → 6)-glucopyranosyl, and the relative configurations of the two glucopyranosyls were β. Acid hydrolysis (Tanaka et al., 2007) indicated that both glucopyranosyls were D-Glc. Therefore, compound 3 was identified as 1-*O*-*trans*-feruloyl-6-*O*-β-D-glucopyranosyl-β-D-glucopyranoside, and named lycibarbarphenylpropanoid L.

Compound 4 was obtained as a yellowish amorphous powder. The molecular formula of 4 was determined as C₂₁H₂₈O₁₃ by HR-ESI-MS (m/z 511.1425 $[M + Na]^+$; calcd. for C₂₁H₂₈O₁₃Na, 511.1428). The detailed analyses of 1D/2D NMR data of 4 (Table S4, Supporting Information) determined a planar structure consisting of *trans*-p-coumaroyl and two pyranohexose units. A precise comparison of ¹³C NMR data of the sugar unit with those of glycosides recorded in the literature (Bock and Pedersen, 1983; Usui et al., 2017) and the coupling values ($J_{1'-2'} = 7.6$ Hz, $J_{1''-2''} = 7.8$ Hz) indicated that the sugar chain of 4 was glucopyranosyl-(1 → 6)-glucopyranosyl, and the relative configurations

Table 1
NMR data of **1–4** (δ in ppm, J in Hz).

No.	1 ^b		2 ^b		3 ^c		4 ^c	
	δ_C	δ_H^a	δ_C	δ_H^a	δ_C	δ_H^a	δ_C	δ_H^a
1	127.3		127.3		127.5		127.0	
2	131.2	7.46, d (8.6)	131.3	7.47, d (8.6)	111.9	7.19, br s	131.4	7.48, d (8.7)
3	116.8	6.80, d (8.6)	116.8	6.80, d (8.6)	149.4		116.9	6.81, d (8.7)
4	161.2		161.2		150.9		161.6	
5	116.8	6.80, d (8.6)	116.8	6.80, d (8.6)	116.5	6.81, d (8.1)	116.9	6.81, d (8.7)
6	131.2	7.46, d (8.6)	131.3	7.47, d (8.6)	124.4	7.09, br d (8.1)	131.4	7.48, d (8.7)
7	146.9	7.64, d (15.9)	147.0	7.66, d (15.9)	148.4	7.72, d (16.0)	148.1	7.73, d (15.9)
8	115.3	6.36, d (15.9)	115.1	6.38, d (15.9)	114.7	6.40, d (16.0)	114.4	6.36, d (15.9)
9	168.7		168.8		167.7		167.7	
1'	96.4	4.73, d (8.0)	91.3	5.37, d (3.6)	95.8	5.55, d (7.0)	95.8	5.55, d (7.6)
2'	75.4	4.93, dd (9.5, 8.0)	74.7	4.83	74.0	3.45	74.0	3.41
3'	85.1	3.82	81.3	4.11, dd (9.8, 9.0)	77.7 [*]	3.45	77.8 [*]	3.45
4'	70.2	3.51, dd (9.6, 8.8)	70.1	3.54, dd (9.8, 9.0)	71.0	3.45	71.0	3.45
5'	77.7 [*]	3.40	72.8	3.88	77.9 [*]	3.59	77.8 [*]	3.58
6'	62.6	3.82, Ha	62.5	3.88, Ha	69.5	4.17, dd (11.2, 1.4), Ha	69.5	4.16, dd (11.3, 1.6), Ha
		3.71, dd (12.0, 5.6), Hb		3.75, dd (11.9, 5.0), Hb		3.77, dd (11.2, 5.2), Hb		3.77, dd (11.3, 5.2), Hb
1''	104.8	4.38, d (8.0)	104.9	4.51, d (8.0)	104.5	4.33, d (7.8)	104.5	4.33, d (7.8)
2''	74.7	3.17, dd (9.2, 8.0)	74.8	3.21, dd (9.2, 8.0)	75.1	3.21	75.1	3.20
3''	77.6 [*]	3.27	77.7	3.35	77.8 [*]	3.34	78.0 [*]	3.34
4''	71.3	3.27	71.3	3.30	71.5	3.26	71.5	3.26
5''	78.1	3.30	78.0	3.35	77.9 [*]	3.26	78.0 [*]	3.26
6''	62.6	3.82, Ha	62.5	3.88, Ha	62.7	3.84, dd (12.0, 2.0), Ha	62.7	3.83, dd (12.0, 2.0), Ha
		3.63, dd (11.9, 6.1), Hb		3.66, dd (11.9, 5.8), Hb		3.65, dd (12.0, 5.3), Hb		3.65, dd (12.0, 5.3), Hb
3-OCH ₃					56.5	3.89, s		

* Assignment may be interchanged.

^a The indiscernible signals due to overlap or having the complex multiplicity are reported without designating multiplicity.

^b Measured in CD₃OD (¹H NMR for 600 MHz, ¹³C NMR for 150 MHz).

^c Measured in CD₃OD (¹H NMR for 400 MHz, ¹³C NMR for 100 MHz).

of the two glucopyranosyls were β . Acid hydrolysis (Tanaka et al., 2007) indicated that both glucopyranosyls were D-Glc. Therefore, compound **4** was identified as 1-*O-trans-p*-coumaroyl-6-*O*- β -D-glucopyranosyl- β -D-glucopyranoside, and named lycibarbarphenylpropanoid M.

Compounds **5** and **6** were obtained as a yellowish amorphous powder. The molecular formulas of **5** and **6** were determined as C₂₁H₂₈O₁₃ by HR-ESI-MS (**5**, m/z 511.1427 [M + Na]⁺; **6**, m/z 511.1428 [M + Na]⁺; calcd. for C₂₁H₂₈O₁₃Na, 511.1428). The detailed analyses of 1D/2D NMR data of **5** and **6** (Tables S5 and S6, Supporting Information) determined their planar structures consisting of *trans-p*-coumaric acid and two pyranohexose units. A precise comparison of ¹³C NMR data of the sugar unit with those of glycosides recorded in the literature (Bock and Pedersen, 1983; Veitch et al., 1998; Zi et al., 2008) and the coupling values (**5**, $J_{1'-2'} = 7.7$ Hz, $J_{1''-2''} = 7.8$ Hz; **6**, $J_{1'-2'} = 7.4$ Hz, $J_{1''-2''} = 7.7$ Hz) indicated that the sugar chains of **5** and **6** were glucopyranosyl-(1 \rightarrow 4)-glucopyranosyl and glucopyranosyl-(1 \rightarrow 3)-glucopyranosyl, respectively, and the relative configurations of these

glucopyranosyls were β . Acid hydrolysis (Tanaka et al., 2007) indicated that these glucopyranosyls were D-Glc. Therefore, compounds **5** and **6** were identified as 4-*O*-[β -D-glucopyranosyl-(1 \rightarrow 4)- β -D-glucopyranosyl]-*trans-p*-coumaric acid (named lycibarbarphenylpropanoid N) and 4-*O*-[β -D-glucopyranosyl-(1 \rightarrow 3)- β -D-glucopyranosyl]-*trans-p*-coumaric acid (named lycibarbarphenylpropanoid O), respectively.

The known compounds, 4-*O*-[β -D-glucopyranosyl-(1 \rightarrow 4)- β -D-glucopyranosyl]-*trans*-ferulic acid (**7**, CAS: 919803-07-9) (Table S7, Supporting Information), lycibarbarphenylpropanoid B (**8**, CAS: 1988786-72-6) (Zhou et al., 2017), lycibarbarphenylpropanoid A (**9**, CAS: 1988786-71-5) (Zhou et al., 2017), isosyringoside (**10**, CAS 152686-85-6) (Sugiyama et al., 1993), 4-*O*- β -D-glucopyranosyl-*trans*-caffeic acid (**11**, CAS: 147511-61-3) (Nyandat et al., 1993), 3-*O*- β -D-glucopyranosyl-*trans*-caffeic acid (**12**, CAS: 143729-78-6) (Table S8, Supporting Information), 4-*O*- β -D-glucopyranosyl-*trans-p*-coumaric acid (**13**, CAS: 117405-49-9) (Struijs et al., 2007), 4-*O*- β -D-glucopyranosyl-*cis*-ferulic acid (**14**, CAS: 94942-20-8) (Table S9, Supporting Information), and 4-*O*- β -D-glucopyranosyl-*cis-p*-coumaric acid (**15**, CAS:

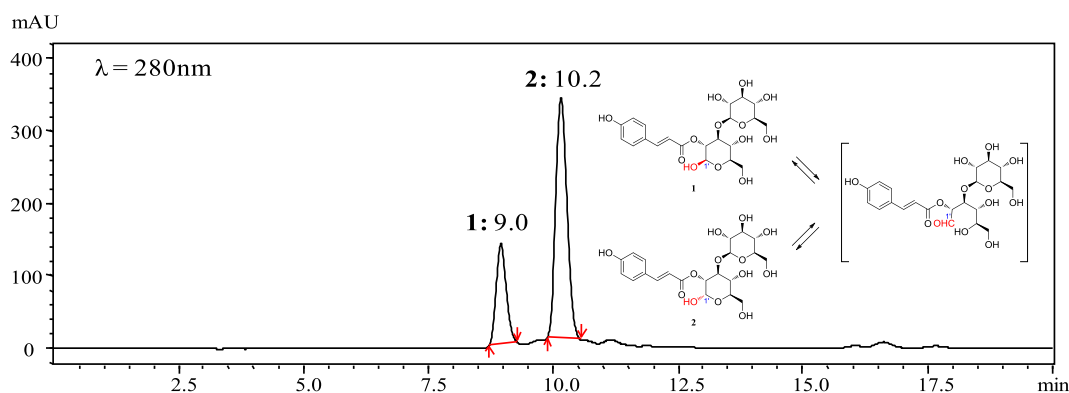


Fig. 3. The HPLC analytical chromatogram of compounds **1/2** and the tautomerism mechanism due to the hemiacetal at C-1'.

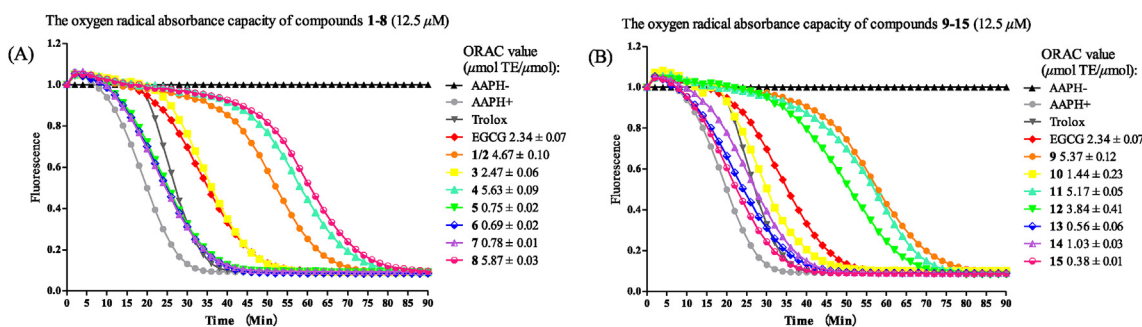


Fig. 4. The antioxidant capacity of compounds 1–15 *in vitro* evaluated by the ORAC method. Each value is expressed as means \pm SE, $n = 4$.

117405-48-8) (Table S10, Supporting Information) were identified by detailed spectroscopic analyses or comparison of their spectroscopic data recorded in the literature. Among them, the 1D and 2D NMR data of compound 7 were firstly reported, and compounds 7 and 10–15 were firstly isolated from the genus *Lycium*.

The antioxidant activities of compounds 1–15 were evaluated using the DPPH radical scavenging assay with vitamin C as the positive control. Only compounds 3 and 12 exhibited moderate DPPH radical scavenging capacity, and the DPPH radical scavenging rate of other compounds were less than 10% (Table S11, Supporting Information).

The antioxidant activities of compounds 1–15 were also evaluated using an ORAC assay. All exhibited different levels of oxygen radical absorbance capacity, and most of the tested compounds exhibited stronger oxygen radical absorbance capacity than EGCG (Fig. 4).

The hypoglycemic activities of compounds 1–15 were evaluated by the α -glucosidase inhibitory assay with acarbose as the positive control. None exhibited potent α -glucosidase inhibitory activity. (Table S13, Supporting Information).

Most carbohydrates found in nature exist as polysaccharides, glycoconjugates, or glycosides, in which sugar units are attached to one another or to aglycones through glycosidic bonds at the anomeric positions (Zhu and Schmidt, 2009; Ati et al., 2017). However, there are special cases, and some rare phenylpropanoid glycosides with free anomeric hydroxy were reported, including 6-*O*-*trans*-sinapoyl- α/β -D-glucopyranoside, 3,6-*O*-dicaffeoyl- α/β -glucopyranoside, and 2,3,4,6-*O*-tetragalloyl- β -D-glucopyranoside (Lou et al., 1993; Kashiwada et al., 1992; Hussein et al., 2003). During this restudy of phytochemical constituents on goji, two unusual glycosides (compounds 1 and 2) characterized by the presence of free anomeric hydroxy were discovered. They were determined to be a pair of inseparable glycosidic anomers in solution, and this phenomenon is rooted in the tautomerism of the hemiacetal at the glucopyranosyls of 1 and 2.

3. Experimental

3.1. General experimental procedures

Optical rotations were recorded on an Anton Paar MCP 200 high precision intelligent polarimeter (Anton Paar Co. Ltd, Graz, Austria). UV data were measured on a JASCO V-550 UV/Vis spectrometer (Jasco International Co. Ltd, Tokyo, Japan). IR data were recorded using a JASCO FT/IR-4600 plus spectrometer. The ESI-MS spectra were recorded on a Bruker amazon SL mass spectrometer (Bruker Daltonics Int., Boston, USA). The HR-ESI-MS spectra were obtained on a Waters Synapt G2 TOF mass spectrometer (Waters Corporation, Milford, USA). The NMR spectra were acquired with Bruker AV 400 and 600 spectrometers (Bruker BioSpin Group, Faellanden, Switzerland) using the solvent signals (DMSO- d_6 : δ_H 2.50/ δ_C 39.5; CD₃OD: δ_H 3.30/ δ_C 49.0) as internal standards. Analytical HPLC was performed on a Dionex HPLC system equipped with an Ultimate 3000 pump, an Ultimate 3000 DAD, an Ultimate 3000 column compartment, an Ultimate 3000 autosampler

(Thermo Fisher Scientific Inc., Sunnyvale, USA), and an Alltech (Grace) 2000 ES ELSD (Alltech Co. Ltd, Portland, USA) using a Phenomenex Gemini C₁₈ column (4.6 \times 250 mm², 5 μ m) (Phenomenex Inc., Los Angeles, USA) and a Cosmosil Packed C₁₈ column (4.6 \times 250 mm², 5 μ m) (Nacalai Tesque Inc., Kyoto, Japan). Semipreparative HPLC was performed on a Dionex HPLC system, which was equipped with an Ultimate 3000 pump and an Ultimate 3000 RS variable wavelength detector using a Phenomenex Gemini C₁₈ column (10.0 \times 250 mm², 5 μ m). Preparative HPLC was performed on a Shimadzu LC-6-AD liquid chromatography system (Shimadzu Inc., Kyoto, Japan) with an SPD-20A detector using a Cosmosil Packed C₁₈ column (20.0 \times 250 mm², 5 μ m). The medium pressure liquid chromatography (MPLC) system was equipped with a dual pump gradient system, an UV preparative detector, and a Dr Flash II fraction collector system (Lisui E-Tech Co. Ltd, Shanghai, China). Column chromatography (CC) was performed on HP-20 macroporous resin (Mitsubishi Chemical Corporation, Tokyo, Japan), silica gel (200–300 mesh, Haiyang Chemical Co. Ltd, Qingdao, China), and ODS (50 μ m, YMC Co. Ltd, Tokyo, Japan).

3.2. Plant material

The fruit of *Lycium barbarum* L. (Solanaceae) was both collected (Zhongning County, Ningxia Hui Autonomous Region, China) and identified by one of the authors (Ying Wang) in 2016. A voucher specimen (LYBA-2016-NX-ZN) was deposited in the Institute of Traditional Chinese Medicine and Natural Products, College of Pharmacy, Jinan University, Guangzhou, China.

3.3. Extraction and isolation

The dried goji (45.0 kg) was cold-soak extracted four times with 100 L of CHCl₃ for 24 h each time. After filtration and evaporation of the CHCl₃, the residue was heated to reflux five times with 120 L of 60% EtOH–H₂O for 2 h each time. After filtration and evaporation of the EtOH *in vacuo*, the concentrated solution was passed through a HP-20 macroporous resin column (20.0 \times 150.0 cm²) using successive elutions of EtOH–H₂O (0:100, 30:70, 50:50, 95:5, v/v), yielding fractions F1–F4.

A portion (900.0 g) of F2 (1.9 kg) was subjected to open silica gel CC (14.0 \times 100.0 cm²) using successive elutions of CHCl₃–MeOH–H₂O (80:20:2, 70:30:3, 60:40:4, 50:50:5, 40:60:6, 0:100:0, v/v/v) to yield fractions 2.1–2.5. Fraction 2.3 (100.0 g) was subjected to ODS-MPLC (5.0 \times 80.0 cm²) using successive elutions of MeOH–H₂O (5:95, 10:90, 15:85, 20:80, 100:0, v/v) to yield fractions 2.3.1–2.3.6. A portion (20.0 g) of fraction 2.3.1 (53.0 g) was subjected to open silica gel CC (5.0 \times 60.0 cm²) using successive elutions of CH₂Cl₂–MeOH–H₂O (85:15:1.5, 80:20:2, 70:30:3, 60:40:4, 50:50:5, 0:100:0, v/v/v) to yield fractions 2.3.1.1–2.3.1.7.

Fraction 2.3.1.3 (683.2 mg) was subjected to MPLC on ODS CC (2.7 \times 12.7 cm²) using successive elutions of MeOH–H₂O–HCOOH (5:95:0.2, 10:90:0.2, 15:85:0.2, 20:80:0.2, 25:75:0.2, 100:0:0, v/v/v) to

yield fractions 2.3.1.3.1–2.3.1.3.6. Fraction 2.3.1.3.3 (145.2 mg) was isolated using semipreparative HPLC [12% MeOH–H₂O (containing 0.2% HCOOH), 3 mL/min] to yield **13** (t_R : 36.5 min, 43.6 mg) and **11** (t_R : 40.2 min, 9.5 mg). Fraction 2.3.1.3.4 (180.1 mg) was isolated using semipreparative HPLC [15% MeOH–H₂O (containing 0.2% HCOOH), 3 mL/min] to yield **15** (t_R : 35.6 min, 112.0 mg) and **12** (t_R : 38.8 min, 13.4 mg). Fraction 2.3.1.3.6 (32.4 mg) was isolated using semipreparative HPLC [20% MeOH–H₂O (containing 0.2% HCOOH), 3 mL/min] to yield **14** (t_R : 30.5 min, 13.4 mg). Fraction 2.3.1.5 (7.5 g) was subjected to MPLC on ODS CC (2.7 × 25.4 cm²) using successive elutions of MeOH–H₂O–HCOOH (5:95:0.2, 10:90:0.2, 15:85:0.2, 20:80:0.2, 25:75:0.2, 100:0:0, v/v/v) to yield fractions 2.3.1.5.1–2.3.1.5.7. Fraction 2.3.1.5.3 (615.8 mg) was isolated using preparative HPLC [10% CH₃CN–H₂O (containing 0.1% CF₃COOH), 8 mL/min] to yield **1/2** (**1**, t_R : 26.1 min; **2**, t_R : 29.6 min; 41.5 mg). Fraction 2.3.1.5.4 (1.09 g) was isolated using semipreparative HPLC [15% MeOH–H₂O (containing 0.2% HCOOH), 3 mL/min] to yield **5** (t_R : 25.4 min, 20.1 mg) and **4** (t_R : 33.8 min, 5.0 mg). Fraction 2.3.1.5.5 (602.3 mg) was isolated using preparative HPLC [8% CH₃CN–H₂O (containing 0.1% CF₃COOH), 10 mL/min] to yield **10** (t_R : 14.5 min, 1.7 mg), **6** (t_R : 33.2 min, 4.2 mg), **3** (t_R : 39.0 min, 30.3 mg), and **8** (t_R : 53.5 min, 87.1 mg). Fraction 2.3.1.5.6 (1.31 g) was isolated using preparative HPLC [9% CH₃CN–H₂O (containing 0.1% CF₃COOH), 8 mL/min] to yield fractions 2.3.1.5.6.1–2.3.1.5.6.7. Fraction 2.3.1.5.6.3 (240.6 mg) was isolated using semipreparative HPLC [15% MeOH–H₂O (containing 0.2% HCOOH), 3 mL/min] to yield **7** (t_R : 52.5 min, 6.5 mg). Fraction 2.3.1.5.6.7 (117.6 mg) was isolated using semipreparative HPLC [22% MeOH–H₂O (containing 0.2% HCOOH), 3 mL/min] to yield **9** (t_R : 29.7 min, 4.1 mg).

3.4. Structural characterization of undescribed compounds

3.4.1. Lycibarbarphenylpropanoids J/K (1/2)

Yellowish amorphous powders; $[\alpha]_D^{25} + 28.0$ (c 0.10, MeOH); UV (MeOH) λ_{max} (log ϵ) 212 (4.22), 229 (4.17), 292 (4.35), 314 (4.45) nm; IR (KBr) ν_{max} 3338, 2908, 1700, 1596, 1513, 1036 cm⁻¹; ESI-MS (positive) m/z 511.2 [M + Na]⁺, 999.2 [2M + Na]⁺; HR-ESI-MS (positive) m/z 511.1426 [M + Na]⁺ (calcd. for C₂₁H₂₈O₁₃Na, 511.1428); ¹H and ¹³C NMR data see Table 1.

3.4.2. Lycibarbarphenylpropanoid L (3)

Yellowish amorphous powder; $[\alpha]_D^{25} - 8.0$ (c 0.10, MeOH); UV (MeOH) λ_{max} (log ϵ) 204 (4.26), 237 (3.91), 295 (3.94), 329 (4.16) nm; IR (KBr) ν_{max} 3294, 2923, 1714, 1596, 1516, 1065 cm⁻¹; ESI-MS (positive) m/z 519.2 [M + H]⁺; HR-ESI-MS (positive) m/z 541.1533 [M + Na]⁺ (calcd. for C₂₂H₃₀O₁₄Na, 541.1533); ¹H and ¹³C NMR data see Table 1.

3.4.3. Lycibarbarphenylpropanoid M (4)

Yellowish amorphous powder; $[\alpha]_D^{25} - 52.0$ (c 0.10, MeOH); UV (MeOH) λ_{max} (log ϵ) 211 (4.08), 230 (4.09), 316 (4.48) nm; IR (KBr) ν_{max} 3300, 2917, 1709, 1604, 1513, 1062 cm⁻¹; ESI-MS (positive) m/z 511.1 [M + Na]⁺, 999.2 [2M + Na]⁺; HR-ESI-MS (positive) m/z 511.1425 [M + Na]⁺ (calcd. for C₂₁H₂₈O₁₃Na, 511.1428); ¹H and ¹³C NMR data see Table 1.

3.4.4. Lycibarbarphenylpropanoid N (5)

Yellowish amorphous powder; $[\alpha]_D^{25} - 48.0$ (c 0.10, MeOH); UV (MeOH) λ_{max} (log ϵ) 208 (4.29), 221 (4.15), 285 (4.29), 306 (4.14) nm; IR (KBr) ν_{max} 3184, 2884, 1697, 1604, 1513, 1080 cm⁻¹; ESI-MS (positive) m/z 489.2 [M + H]⁺, 977.3 [2M + H]⁺; HR-ESI-MS (positive) m/z 511.1427 [M + Na]⁺ (calcd. for C₂₁H₂₈O₁₃Na, 511.1428); ¹H and ¹³C NMR data see Table 2.

3.4.5. Lycibarbarphenylpropanoid O (6)

Yellowish amorphous powder; $[\alpha]_D^{25} - 14.0$ (c 0.10, MeOH); UV

Table 2
NMR data of **5**–**7** (δ in ppm, J in Hz).

No.	5 ^b		6 ^b		7 ^b	
	δ_C	δ_H^a	δ_C	δ_H^a	δ_C	δ_H^a
1	128.6		128.4		128.3, C	
2	129.4	7.58, d (8.6)	129.7	7.60, d (8.5)	111.2, CH	7.33, d (1.0)
3	116.4	7.04, d (8.6)	116.5	7.05, d (8.5)	149.1, C	
4	158.4		158.6		148.2, C	
5	116.4	7.04, d (8.6)	116.5	7.05, d (8.5)	114.9, CH	7.10, d (8.5)
6	129.4	7.58, d (8.6)	129.7	7.60, d (8.5)	122.1, CH	7.18, dd (8.5, 1.0)
7	141.6	7.44, d (15.8)	142.7	7.48, d (15.9)	143.8, CH	7.52, d (15.9)
8	119.8	6.39, d (15.8)	118.5	6.39, d (15.9)	117.4, CH	6.46, d (15.9)
9	168.9		168.4		167.9, C	
1'	99.6	5.02, d (7.7)	99.3	5.07, d (7.4)	99.1, CH	5.06, d (7.8)
2'	72.9	3.31, t (8.0)	72.0	3.47	72.8, CH	3.32
3'	74.8	3.46	87.6	3.51	75.1 [*] , CH	3.44
4'	79.8	3.44	68.1	3.32, t (8.6)	79.8, CH	3.44
5'	75.0	3.56	76.5	3.45	75.0 [*] , CH	3.54
6'	60.0	3.75, br d (12.2), Ha	60.5	3.70, Ha	60.0	3.72, br d (11.6), Ha
		3.64, dd (12.0, 4.3), Hb		3.49, Hb		3.64, Hb
1''	103.1	4.30, d (7.8)	104.0	4.36, d (7.7)	103.1, CH	4.29, d (7.8)
2''	73.3	3.02, t (8.4)	73.9	3.09	73.3, CH	3.02
3''	76.5	3.19	76.1	3.20	76.5, CH	3.20
4''	70.0	3.07, t (9.2)	70.2	3.05	70.0, CH	3.07
5''	76.8	3.19	77.0	3.20	76.8, CH	3.20
6''	61.0	3.71, br d (12.5), Ha	61.1	3.70, Ha	61.0	3.72, br d (11.6), Ha
		3.42, Hb		3.40, dd (11.7, 7.0), Hb		3.42, Hb
3-OCH ₃					56.5, CH ₃	3.81, s
2'-OH						5.44, d (5.8)
3'-OH						4.80, br s
6'-OH						4.62
2'''-OH						5.24, d (3.0)
3'''-OH						5.01, br s
4'''-OH						5.01, br s
6'''-OH						4.62

* Assignment may be interchanged.

^a The indiscernible signals due to overlap or having the complex multiplicity are reported without designating multiplicity.

^b Measured in DMSO-*d*₆ (¹H NMR for 400 MHz, ¹³C NMR for 100 MHz).

(MeOH) λ_{max} (log ϵ) 207 (4.03), 220 (3.95), 285 (4.13), 306 (4.00) nm; IR (KBr) ν_{max} 3300, 2917, 1685, 1604, 1513, 1077 cm⁻¹; ESI-MS (positive) m/z 489.2 [M + H]⁺, 977.1 [2M + H]⁺; HR-ESI-MS (positive) m/z 511.1428 [M + Na]⁺ (calcd. for C₂₁H₂₈O₁₃Na, 511.1428); ¹H and ¹³C NMR data see Table 2.

3.5. Acid hydrolysis

The acid hydrolysis was performed using a previously described method with slight modifications (Tanaka et al., 2007). The compound (1.0 mg) was hydrolyzed with 2 M of HCl for 1 h at 90 °C. After extraction with EtOAc two times, the H₂O layer was evaporated *in vacuo* using an Eyela N-1001 rotary evaporator (Tokyo Rikakikai Co. Ltd, Tokyo, Japan) to furnish a monosaccharide residue. The residue was dissolved in pyridine (1.0 mL) containing L-cysteine methyl ester hydrochloride (1.0 mg) and heated at 60 °C. After 1 h, 20 μ L of *o*-tolyl isothiocyanate was added to the reaction mixture and further reacted at 60 °C for 3 h. Then the reaction mixture was directly analyzed by the Dionex HPLC system and detected by a UV detector (at 250 nm). The standard monosaccharides of D-Glc and L-Glc were subjected to the same method.

3.6. DPPH radical scavenging assay

The DPPH radical scavenging assay was performed based on the method with slight modifications (Cardullo et al., 2019; Xie et al., 2015; Hidayat et al., 2017; Lu et al., 2017). In a 96-well plate, 100 μ L of 0.2 mM DPPH radical solution in ethanol was added to 100 μ L of the 0.2 mM sample solutions in ethanol. The mixture was wobbled for 30 min in the dark. Vitamin C was used as a positive control. The absorbance values were measured at 517 nm using a Synergy HT microplate reader (Bio-Tek Instruments Inc., Burleigh, USA). All of the samples were performed in triplicate. The DPPH radical scavenging rate (%) was calculated as follows: $S\% = [(A_0 - A_1) / A_0] \times 100$ (A_1 and A_0 are the absorbance of the incubation DPPH radical solution with and without the tested sample, respectively).

3.7. Oxygen radical absorbance capacity (ORAC) assay

The ORAC assay was performed in accordance with the previously described method (Cardullo et al., 2019; Zhang et al., 2016). The automated ORAC assay was carried out on a GENios Luciferase-based microplate reader (Tecan Group Ltd, Männedorf, Switzerland) with an excitation/emission filter pair of 485/527 nm. Sodium fluorescein was used as a fluorescence probe, and the reaction was initiated with the addition of AAPH. EGCG was used as a positive control. The results were calculated using the difference in the area under the fluorescence decay curve between the AAPH control and each sample. The ORAC values of the tested samples were calculated as the relative values of the area under the fluorescence decay curve using Trolox as a standard, and expressed as micromoles of Trolox equivalents (TE) per micromoles of sample (μ mol TE/ μ mol). All samples were analyzed in quadruplicate.

3.8. α -Glucosidase inhibitory assay

The α -glucosidase inhibitory activity was performed according to the previously described procedure with slight modifications (Cardullo et al., 2019; Omar et al., 2012; Boue et al., 2016). Briefly, 25 μ L of 1.6 mM tested samples were put into 96-well microplate followed by 50 μ L of 0.6 U/mL α -glucosidase solution (Sigma-Aldrich Chemical Co. Ltd, Saint Louis, USA) and then preincubated for 10 min at 37 °C. Then, a 25 μ L of 5 mM *p*-NPG was added into each well and incubated for 5 min at 37 °C. After 5 min of incubation at 37 °C, 100 μ L of 0.1 M Na₂CO₃ was added into each well to terminate the reaction. The absorbance values were measured at 405 nm using a Synergy HT microplate reader. Acarbose was used as a positive control. All samples were analyzed in triplicate. The relative inhibitory activity (%) was calculated as follows: $I\% = [(E - S) / E] \times 100$ (E and S are the absorbance of the incubated α -glucosidase solution without and with the tested sample, respectively).

3.9. Statistical analysis

The data were plotted using GraphPad Prism 5.01 software, and expressed as means \pm SE. One-way analysis of variance (ANOVA) (SPSS, Version 15, USA) was applied to analyze for differences in data of biochemical parameters, followed by Dunnett Post Hoc test (all compounds vs positive control).

Acknowledgements

This work was financially supported by grants from the National Natural Science Foundation of China (3171101305, 81703372, and 81703696), Chang Jiang Scholars Program (Hao Gao, 2017) from the Ministry of Education of China, Guangdong Special Support Program (2016TX03R280), Guangdong Province Universities and Colleges Pearl River Scholar Funded Scheme (Hao Gao, 2014), Local Innovative and Research Teams Project of Guangdong Pearl River Talents Program

(2017BT01Y036), and K. C. Wong Education Foundation (Hao Gao, 2016). Assistance with Scientific English was provided by Dr L.J. Sparvero of the University of Pittsburgh.

Appendix A. Supplementary data

Supplementary data to this article can be found online at <https://doi.org/10.1016/j.phytochem.2019.04.017>.

References

- Amagase, H., Farnsworth, N.R., 2011. A review of botanical characteristics, phytochemistry, clinical relevance in efficacy and safety of *Lycium barbarum* fruit (Goji). *Food Res. Int.* 44, 1702–1717.
- Ati, J., Lafite, P., Daniellou, R., 2017. Enzymatic synthesis of glycosides: from natural O- and N-glycosides to rare C- and S-glycosides. *Beilstein J. Org. Chem.* 13, 1857–1865.
- Bock, K., Pedersen, C., 1983. Carbon-13 nuclear magnetic resonance spectroscopy of monosaccharides. *Adv. Carbohydr. Chem. Biochem.* 41, 27–66.
- Boue, S.M., Daigle, K.W., Chen, M.H., Cao, H.P., Heiman, M.L., 2016. Antidiabetic potential of purple and red rice (*Oryza sativa* L.) bran extracts. *J. Agric. Food Chem.* 64, 5345–5353.
- Cardullo, N., Catinella, G., Floresta, G., Muccilli, V., Rosselli, S., Rescifina, A., Bruno, M., Tringali, C., 2019. Synthesis of rosmarinic acid amides as antioxidative and hypoglycemic agents. *J. Nat. Prod.* <https://doi.org/10.1021/acs.jnatprod.8b01002>.
- Chen, S.D., Li, T., Gao, H., Zhu, Q.C., Lu, C.J., Wu, H.L., Peng, T., Yao, X.S., 2013. Anti HSV-1 flavonoid derivatives tethered with houttuynin from *Houttuynia cordata*. *Planta Med.* 79, 1742–1748.
- Gao, H., Yao, X.S., 2019. Strengthen the research on the medicinal and edible substances to advance the development of the comprehensive healthcare industry of TCMs. *Chin. J. Nat. Med.* 17, 1–2.
- Hidayat, M.A., Fitri, A., Kuswandi, B., 2017. Scanometry as microplate reader for high throughput method based on DPPH dry reagent for antioxidant assay. *Acta Pharm. Sin.* 38, 395–400.
- Hussein, S.A.M., Ayoub, N.A., Nawwar, M.A.M., 2003. Caffeoyl sugar esters and an elagitannin from *Rubus sanctus*. *Phytochemistry* 63, 905–911.
- Kashiwada, Y., Nonaka, G.I., Nishioka, I., Chang, J.J., Lee, K.H., 1992. Antitumor agents, 129. Tannins and related compounds as selective cytotoxic agents. *J. Nat. Prod.* 55, 1033–1043.
- Kulkarni, S.S., Wang, C.C., Sabbavarapu, N.M., Podilapu, A.R., Liao, P.H., Hung, S.C., 2018. “One-pot” protection, glycosylation, and protection–glycosylation strategies of carbohydrates. *Chem. Rev.* 118, 8025–8104.
- Lou, H.X., Li, X., Zhu, T.R., Li, W., 1993. Sinapic acid esters and a phenolic glycoside from *Cynanchum hancockianum*. *Phytochemistry* 32, 1283–1286.
- Lu, Y.Y., Gong, X.P., Xue, Y.B., Zhu, H.C., Li, X.N., Hu, L.Z., Guan, J.K., Zhang, J.W., Du, G., Zhang, Y.H., 2017. Two pairs of chlorine-containing phenylpropanoid enantiomers from *Acorus tatarinowii*. *Chin. Chem. Lett.* 28, 1460–1464.
- Nyandat, E., Rwekika, E., Galeffi, C., Palazzino, G., Nicoletti, M., 1993. Olinioside, 5-(4'-O- β -D-glucopyranosyl)-caffeoyloxy-5,6-dihydro-4-methyl-(2H)-pyran-2-one from *Olinia usambarensis*. *Phytochemistry* 33, 1493–1496.
- Omar, R., Li, L., Yuan, T., Seeram, N.P., 2012. α -Glucosidase inhibitory hydrolyzable tannins from *Eugenia jambolana* seeds. *J. Nat. Prod.* 75, 1505–1509.
- Qian, D., Zhao, Y.X., Yang, G., Huang, L.Q., 2017. Systematic review of chemical constituents in the genus *Lycium* (Solanaceae). *Molecules* 22, 911.
- Struijs, K., Vincken, J.P., Verhoef, R., van Oostveen-van Casteren, W.H.M., Voragen, A.G.J., Gruppen, H., 2007. The flavonoid herbacetin diglucoside as a constituent of the lignan macromolecule from flaxseed hulls. *Phytochemistry* 68, 1227–1235.
- Sugiyama, M., Nagayama, E., Kikuchi, M., 1993. Lignan and phenylpropanoid glycosides from *Osmanthus asiaticus*. *Phytochemistry* 33, 1215–1219.
- Sun, T.Y., Kuang, R.Q., Chen, G.D., Qin, S.Y., Wang, C.X., Hu, D., Wu, B., Liu, X.Z., Yao, X.S., Gao, H., 2016. Three pairs of new isopentenyl dibenzo[b,e]oxepinone enantiomers from *Talaromyces flavus*, a wetland soil-derived fungus. *Molecules* 21, 1184.
- Tanaka, T., Nakashima, T., Ueda, T., Tomii, K., Kouno, I., 2007. Facile discrimination of aldose enantiomers by reversed-phase HPLC. *Chem. Pharm. Bull.* 55, 899–901.
- Usui, A., Matsuo, Y., Tanaka, T., Ohshima, K., Fukuda, S., Mine, T., Yakashiro, I., Ishimaru, K., 2017. Ferulic acid esters of glucosylglucose from *Allium macrostemon* Bunge. *J. Asian Nat. Prod. Res.* 19, 215–221.
- Veitch, N.C., Grayer, R.J., Irwin, J.L., Takeda, K., 1998. Flavonoid cellobiosides from *Sabia uliginosa*. *Phytochemistry* 48, 389–393.
- Wojdyło, A., Nowicka, P., Bąbelewski, P., 2018. Phenolic and carotenoid profile of new goji cultivars and their antihyperglycemic, anti-aging and antioxidant properties. *J. Funct. Foods* 48, 632–642.
- Xie, J.H., Dong, C.J., Nie, S.P., Li, F., Wang, Z.J., Shen, M.Y., Xie, Y.M., 2015. Extraction, chemical composition and antioxidant activity of flavonoids from *Cyclocarya paliurus* (Batal.) Iljinskaja leaves. *Food Chem.* 186, 97–105.
- Yang, Y., Zhang, X.H., Yu, B., 2015. O-Glycosylation methods in the total synthesis of complex natural glycosides. *Nat. Prod. Rep.* 32, 1331–1355.
- Zhang, X.X., Ma, S.C., Mao, P., Wang, Y.D., 2016. A new bisbenzylisoquinoline alkaloid from *Plumulanelumbinis*. *Chin. Chem. Lett.* 27, 1755–1758.
- Zhou, Z.Q., Fan, H.X., He, R.R., Sun, W.Y., Xiao, J., Bao, X.F., So, K.F., Yao, X.S., Gao, H., 2016a. Four new dicafeoylspermidine derivatives from *Lycium barbarum*. *World J. Tradit. Chin. Med.* 2, 1–5.

- Zhou, Z.Q., Fan, H.X., He, R.R., Xiao, J., Tsoi, B., Lan, K.H., Kurihara, H., So, K.F., Yao, X.S., Gao, H., 2016b. Lycibarbarspermidines A–O, new dicaffeoylspermidine derivatives from wolfberry, with activities against Alzheimer's disease and oxidation. *J. Agric. Food Chem.* 64, 2223–2237.
- Zhou, Z.Q., Xiao, J., Fan, H.X., Yu, Y., He, R.R., Feng, X.L., Kurihara, H., So, K.F., Yao, X.S., Gao, H., 2017. Polyphenols from wolfberry and their bioactivities. *Food Chem.* 214, 644–654.
- Zhu, X.M., Schmidt, R.R., 2009. New principles for glycoside-bond formation. *Angew. Chem. Int. Ed.* 48, 1900–1934.
- Zi, J.C., Li, S., Liu, M.T., Gan, M.L., Lin, S., Song, W.X., Zhang, Y.L., Fan, X.N., Yang, Y.C., Zhang, J.J., Shi, J.G., Di, D.L., 2008. Glycosidic constituents of the tubers of *Gymnadenia conopsea*. *J. Nat. Prod.* 71, 799–805.